SLAC – PUB – 4011
DPNU – 86 – 18
June 1986
T/E

OBSERVATION OF THE LEADING K^* L–EXCITATION SERIES FROM $J^P = 1^-$ THROUGH 5^- IN THE REACTION $K^- p \to K^- \pi^+ n$ AT 11 GeV/c*

D. Aston,[a] *N. Awaji,*[b] *J. D'Amore,*[c] *W. Dunwoodie,*[a] *R. Endorf,*[c] *K. Fujii,*[b‡] *H. Hayashii,*[b**] *S. Iwata,*[b‡] *W.B. Johnson,*[a] *R. Kajikawa,*[b] *P. Kunz,*[a] *D.W.G.S. Leith,*[a] *L. Levinson,*[a§§] *T. Matsui,*[b‡] *B.T. Meadows,*[c] *A. Miyamoto,*[b‡] *M. Nussbaum,*[c] *H. Ozaki,*[b] *C.O. Pak,*[b‡] *B.N. Ratcliff,*[a] *D. Schultz,*[a] *S. Shapiro,*[a] *T. Shimomura,*[b] *P. K. Sinervo,*[a†] *A. Sugiyama,*[b] *S. Suzuki,*[b] *G. Tarnopolsky,*[a♯] *T. Tauchi,*[b‡] *N. Toge,*[a] *K. Ukai,*[d] *A. Waite,*[a] *S. Williams*[a♯♯]

[a] *Stanford Linear Accelerator Center, Stanford University, P.O. Box 4349, Stanford, California 94305*
[b] *Department of Physics, Nagoya University, Furo-cho, Chikusa-ku, Nagoya 464, Japan*
[c] *University of Cincinnati, Cincinnati, Ohio 45221*
[d] *Institute of Nuclear Study, University of Tokyo, 3-2-1 Midori-cho, Tanashi-shi, Tokyo 188, Japan*

ABSTRACT

High statistics data for the reaction $K^- p \to K^- \pi^+ n$ at 11 GeV/c have been obtained in the LASS spectrometer at SLAC. A spherical harmonic moments analysis provides clear evidence for the production of the complete leading orbitally excited K^* series up through $J^P = 5^-$. New measurements are made of the masses and widths of the 1^- $K^*(892)$, 2^+ $K^*(1430)$, 3^- $K^*(1780)$, and 4^+ $K^*(2060)$, and evidence is presented for the production of a new K^* state at 2382 MeV/c^2 with spin-parity 5^-.

Submitted to *Physics Letters B*

* Work supported in part by the Department of Energy under contract No. DE-AC03-76SF00515; the National Science Foundation under grant No. PHY82-09144, and the Japan U.S. Cooperative Research Project on High Energy Physics.

‡ Present Address: National Laboratory for High Energy Physics, KEK, Oho-machi, Tsukuba, Ibaraki 305, Japan.
** Present Address: Nara Women's University, Kitauoya-nishi-machi, Nara-shi, Nara 630, Japan.
§§ Present Address: Weizmann Institute, Rehovot 76100, Israel.
† Present Address: University of Pennsylvania, Philadelphia, Pennsylvania 19104, U.S.A.
♯ Present Address: Hewlett-Packard Laboratories, 1501 Page Mill Road, Palo Alto, California 94304, U.S.A.
♯♯ Present Address: Diasonics Corp., 533 Cabot Rd., S. San Francisco, CA 94090, U.S.A.

Previous studies of the reaction

$$K^- p \rightarrow K^- \pi^+ n \tag{1}$$

have proved to be especially fruitful in elucidating the structure of the strange meson system. This final state is topologically very simple, contains contributions from only natural spin-parity meson decays, and has a large cross section which is dominated by π exchange at small values of momentum transfer ($t' = t - t_{min}$) [1]. These features have allowed clear observations to be made of the three lowest-mass orbitally (L) excited K^* states [the spin-parity 1^- $K^*(892)$, the 2^+ $K^*(1430)$, and the 3^- $K^*(1780)$]; in addition, evidence for the next L-excitation, the 4^+ $K^*(2060)$ [1–3] has been obtained. However, at higher mass, the increasingly inelastic nature of $K\pi$ scattering, coupled with experimental limitations of acceptance and sensitivity, has prevented any observation of the continuation of the L-excitation series which is predicted by the quark model. In this paper, results are presented from a spherical harmonic moments analysis of the $K^-\pi^+$ system in reaction (1) using new high statistics (4 events/nb) data at 11 GeV/c incident momentum obtained with the LASS spectrometer at SLAC. New measurements of the masses and widths of the 1^- $K^*(892)$, 2^+ $K^*(1430)$, 3^- $K^*(1780)$, and 4^+ $K^*(2060)$ are made, and evidence is presented for a new 5^- K^* state.

The LASS spectrometer contains a superconducting solenoid vertex detector, a downstream dipole spectrometer and a variety of charged particle detectors, as discussed in detail in ref. 4. The spectrometer provides nearly 4π geometrical acceptance with good momentum resolution for a wide range of momenta. The trigger system for this experiment is designed to accept nearly all events with two or more charged secondaries emerging from the target and is defined by requiring two or more hits in PWC detectors which surround the target.

After event reconstruction, candidates for reaction (1) are chosen from the two prong, charge-zero events by requiring the missing mass squared of the recoil system to lie between 0.5 and 1.2 (GeV/c^2)^2. Elastic K^-p, K^0, Λ, and ϕ events are explicitly rejected. The remaining backgrounds come primarily from the reactions $K^-p \rightarrow K^-\pi^+\Delta^0$ and $K^-p \rightarrow K^-\pi^0 p$, and are estimated to be 6% of the neutron sample. The selection yields a sample of 730,000 events with $|t'| \leq 1.0$ (GeV/c)^2.

In addition to the forward production of K^* mesons, there is also substantial production of N^* systems in the region of low $n\pi^+$ invariant mass. To avoid reflections from this region, events with an $n\pi^+$ mass below 1.7 GeV/c^2 are removed for the subsequent analysis. The remaining sample contains 385,000 events.

The resulting $K^-\pi^+$ invariant mass is shown in fig. 1. The $K^*(892)$ and $K^*(1430)$ mesons can be clearly seen as can a higher mass structure in the $K^*(1780)$ region. However, the large number of overlapping resonances at higher mass leads to a rather featureless distribution above 2.0 GeV/c^2. Information about these resonances can be extracted from the decay angular distribution. For the angular analysis, events with $|t'| \leq 0.2$ (GeV/c)^2 are chosen in order to enhance the pion exchange component. In fig. 2 the scatter plot of $K^-\pi^+$ invariant mass against the cosine of the helicity angle in the t-channel helicity (Gottfried–Jackson) frame is shown. Clear bands corresponding to the $K^*(892)$ and $K^*(1430)$ are evident but other complicated structures are also apparent; these are due to interference effects and their interpretation requires a detailed angular analysis. The final data sample used for analysis contains 151,000 events in the mass region below 2.6 GeV/c^2 with $|t'| \leq 0.2$ (GeV/c)^2.

The geometrical acceptance of LASS covers most of the 4π solid angle but Monte Carlo acceptance corrections are still required to account for any non-uniformities in the spectrometer geometry and trigger, decay and absorption of particles, resolution and efficiency of detectors, and the cuts applied in defining the data sample. The same reconstruction and event selection programs are applied to the Monte Carlo events and to the real data.

The acceptance corrected spherical moments ($t_L^M = \sqrt{4\pi}\, N \langle Y_{LM} \rangle$) in the t channel helicity frame are obtained by the extended maximum likelihood method. The number of moments required to fit the $K^-\pi^+$ angular distributions is found to increase with $K\pi$ mass. In general, in order to minimize the correlation between moments which arises from non-uniformities in the acceptance, a minimum set of moments $M \leq M_{max}$, $L \leq L_{max}$ is used in each mass region, where M_{max} and L_{max} are the smallest maximum values required by the data. Higher moments, if included, do not alter the quality of the fit. However, the correlations do substantially increase the error bars on all moments if unnecessary higher moments are included.

Due to the dominance of π-exchange in reaction (1), the largest moments have $M = 0$ and resonances with spin J appear in moments with L up to $2J$. Figure 3 shows the even L, $M = 0$ moments required to describe the data in the mass region below 1.88 GeV/c^2. The 1^- $K^*(892)$, 2^+ $K^*(1430)$, and 3^- $K^*(1780)$ are clearly seen in the t_2^0, t_4^0, and t_6^0 moments, respectively. Each state dominates the highest moment required in the relevant mass region, demonstrating the well-known spin-parities of these states. Measurements of their masses and widths are obtained by performing a fit to the resonance peak as observed in the $L = 2J$ moment using a relativistic Breit-Wigner parametrization of the form† $|BW|^2$, where

† The on-shell form used here is equivalent to the modified off-shell Breit-Wigner form derived by J.Pisut and M.Roos [5] which has been applied extensively in other reactions dominated by pion exchange.

$$BW = N_L \cdot \left(\frac{M_{K\pi}}{\sqrt{q}}\right) \frac{M_L \Gamma}{(M_L^2 - M_{K\pi}^2) - iM_L\Gamma_{tot}} \quad , \tag{2}$$

M_L is the resonance mass, $M_{K\pi}$ is the invariant mass of the $K\pi$ system, N_L is a normalization constant, and q is the momentum in the $K\pi$ center-of-mass. The mass-dependent width Γ_{tot} is given by

$$\Gamma_{tot} = \Gamma_L \left(\frac{q}{q_L}\right)^{2L+1} \frac{D_L(q_L R)}{D_L(qR)} \left(\frac{M_L}{M_{K\pi}}\right) \quad , \tag{3}$$

where Γ_L is the width of the resonance, q_L is evaluated at the resonance mass, and $D_L(qR)$ is the barrier factor defined by Blatt and Weisskopf [6]. The same mass and q dependence are given to Γ_{tot} and Γ. The resulting fits are indicated by the solid lines in fig. 3, and the masses and resolution-corrected widths are summarized in table I. Additional fits were performed in which the mass regions were changed or where an additional linear background term was added to the amplitude. The variation in the parameter values obtained with these additional fits is used to define the systematic errors indicated in table I.

All of the required moments for the $K^-\pi^+$ mass region above 1.8 GeV/c^2 are shown in fig. 4. The high moments are plotted in overlapping bins to guide the eye. Moments with $M \geq 2$ or $L \geq 11$ are not required to fit the data and are therefore not included in the fit to determine the moments with $L \leq 10$ which are displayed. However, when included, the $L = 11$ and 12 moments (also shown in fig. 4) are structureless and consistent with zero indicating that the maximum amplitude required by the data is the H wave. The peaks in the t_8 and t_{10} moments and the interference patterns seen in the t_7 and t_9 moments are naturally interpreted as indicating the presence of spin–4 and spin–5 leading K^* resonances. However, the large errors make it difficult to determine the resonance parameters from the leading moments alone. Hence, a simple mass dependent fit of all the moments has been performed to obtain estimates of the resonance parameters of these observed structures.

Table I

Leading K^* Resonance Parameters. The parameters for the 1^-, 2^+, and 3^- states come from the fit to the leading moments. The 4^+ and 5^- parameters come from the fit to all the high mass moments. The indicated errors are statistical and systematic, respectively.

Resonance	J^P	Mass (MeV/c^2)	Width (MeV/c^2)
$K^*(892)$	1^-	$897.0 \pm 0.7 \pm 0.7$	$49.9 \pm 1.7 \pm 0.8$
$K^*(1430)$	2^+	$1433.0 \pm 1.6 \pm 0.5$	$115.8 \pm 2.7 \pm 1.6$
$K^*(1780)$	3^-	$1778.1 \pm 6.4 \pm 1.3$	$185.9 \pm 23.3 \pm 12.3$
$K^*(2060)$	4^+	$2062 \pm 14 \pm 13$	$221 \pm 48 \pm 27$
$K^*(2380)$	5^-	$2382 \pm 14 \pm 19$	$178 \pm 37 \pm 32$

The basic assumptions of this analysis are chosen to be consistent with the standard PWA analysis models [7] and with earlier energy independent PWA's of reaction (1) [1]. The dominant structures are assumed to arise from resonating partial waves with spin 3, 4 and 5 parametrized as relativistic Breit-Wigner forms as in expression (2). The parameters for the $K^*(1780)$ are fixed on the basis of the previous t_6^0 moment fit. The lower spin (S, P, D, F) helicity–0 waves include coherent background terms parametrized as first order polynomials in $K^-\pi^+$ mass according to

$$L_0^{BG} = (N_0^L + N_1^L M_{K\pi}) e^{i(\phi_0^L + \phi_1^L M_{K\pi})} \tag{4}$$

A similar background form is used for the G wave with the additional requirement that L_0^{BG} is set to zero below a 2.0 GeV/c^2 threshold mass. For the helicity–1 amplitude, the parametrization [8].

$$L_1^{\pm} = \sqrt{L(L+1)/2} \cdot \frac{C}{1 - B \cdot M_{K\pi}^2} \cdot L_0$$

is assumed, where B and C are parameters to be fitted.

These amplitudes are transformed into moments and fit by minimizing the resulting χ^2 function obtained using the complete error matrix and the data from the non-overlapping bins indicated by the solid points in fig. 4. The results of the fit are displayed as solid curves in the figure. The quality of the fit is excellent (χ^2/NDF=112/144), and the resonance parameter values obtained are summarized in Table I. Including second order terms in the polynomial background does not improve the fit (χ^2/NDF=107/136). In order to demonstrate that the H wave requires a resonant shape and is not simply due to a rising amplitude, a conservative estimate of significance is obtained by adding a five parameter linear background (similar to the G wave form but with an arbitrary mass threshold) to the H wave amplitude parametrization. The significance of the H wave resonance in this model is 4.7 σ. However,when the H wave background term is added, relatively large correlations appear which affect the resonance parameters significantly. Changes in the resonance parameters also occur when different mass binnings are used and when other forms are used for the lower spin amplitudes. These model-dependent variations are taken into account in the systematic errors indicated in table I.

In conclusion, new measurements of the resonance parameters of the first four leading K^* resonances have been presented and clear evidence for a new $J^P = 5^-$ K^* resonance at a mass of 2382 MeV/c^2 with a width of 178 MeV/c^2 has been obtained. This state is most naturally interpreted as a continuation of the L-excitation ladder predicted by the quark model, and as the $I = 1/2$ SU(3) partner of a previously reported $I = 1$, $J^P = 5^-$ state, the $\rho(2310)$ [9].

We are very grateful for the support of the technical staffs of SLAC Group B and Nagoya University.

REFERENCES

[1]. P. Estabrooks et al., Phys. Lett. 60B (1976) 473.

P. Estabrooks et al., Nucl. Phys. 133B (1978) 490.

D. Aston et al., Phys. Lett. 106B (1981) 235.

[2]. D. Aston et al., Phys. Lett. 99B (1981) 502.

W.E.Cleland et al., Phys. Lett. 97B (1980) 465.

[3]. See, for example, Review of Particle Properties, Particle Data Group, Rev. Mod. Phys. 56 (1984), and references therein.

[4]. D. Aston et al., The LASS Spectrometer, SLAC-REPORT 298 (1986).

[5]. J. Pisut and M. Roos, Nucl. Phys. B6 (1968) 325.

[6]. J. Blatt and V. Weisskopf, "Theoretical Nuclear Physics" (Wiley, 1952), p. 361.

[7]. See, for example, $\pi\pi$ Interactions in Particle Physics, B.R. Martin et al., N.Y. Academic Press (1976).

[8]. P. Estabrooks et al., Nucl. Phys. 95B (1975) 322.

[9]. B. Alper et al., Phys. Lett. 94B (1980) 422.

FIGURE CAPTIONS

Figure 1. The $K^-\pi^+$ invariant mass distribution for the data on reaction (1).

Figure 2. The $\cos\theta_{GJ}$ vs. $M_{K\pi}$ scatter plot for events with $|t'| \leq 0.2(GeV/c)^2$; events near $\cos\theta_{GJ} = 1$ at high mass are removed by the N^* and elastic cuts.

Figure 3. The unnormalized L-even, M=0 $K^-\pi^+$ moments for the mass region below 1.88 GeV/c^2; bin sizes vary from 10 to 40 MeV/c^2, with events normalized to 40 MeV/c^2 bins.

Figure 4. The unnormalized $K^-\pi^+$ moments for masses above 1.88 GeV/c^2; bin sizes vary from 80 to 160 MeV/c^2, with events normalized to 40 MeV/c^2 bins. The moments are plotted for overlapping bins; black dots indicate the independent mass bin set used for the fit described in the text.

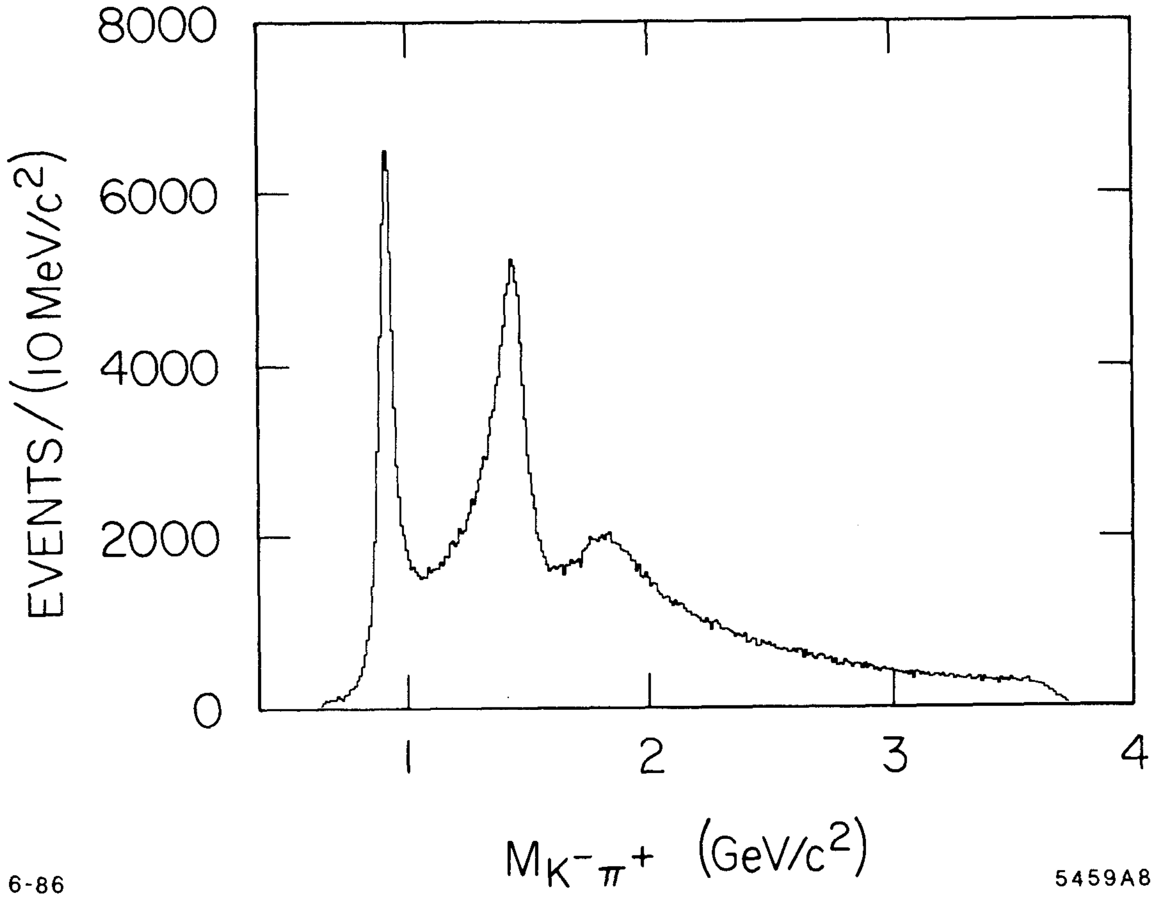

8000
6000
4000
2000
0
EVENTS/(10 MeV/c²)
1
2
3
4
M K⁻π⁺ (GeV/c²)
6-86
5459A8

Fig. 1

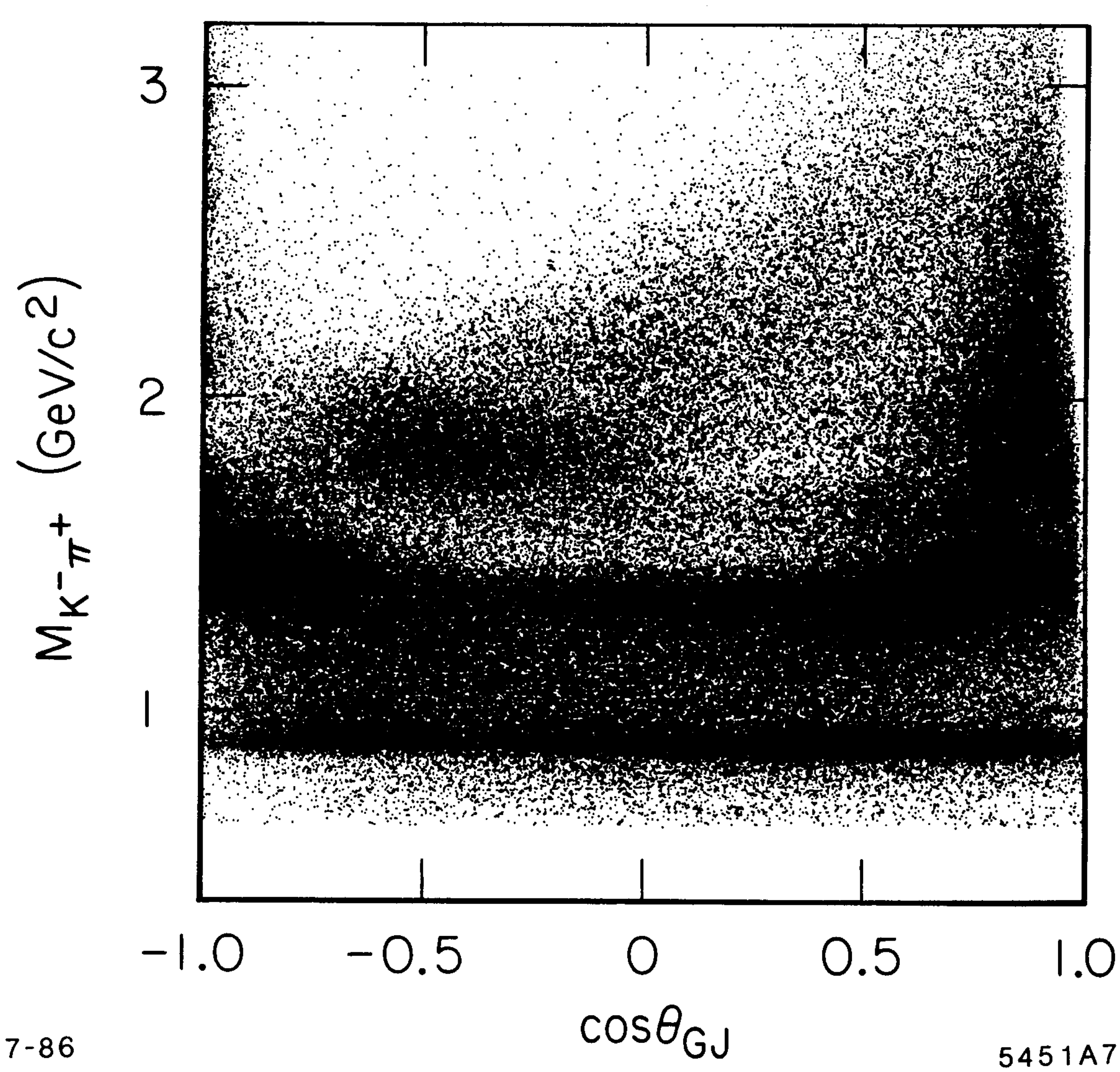

Fig. 2

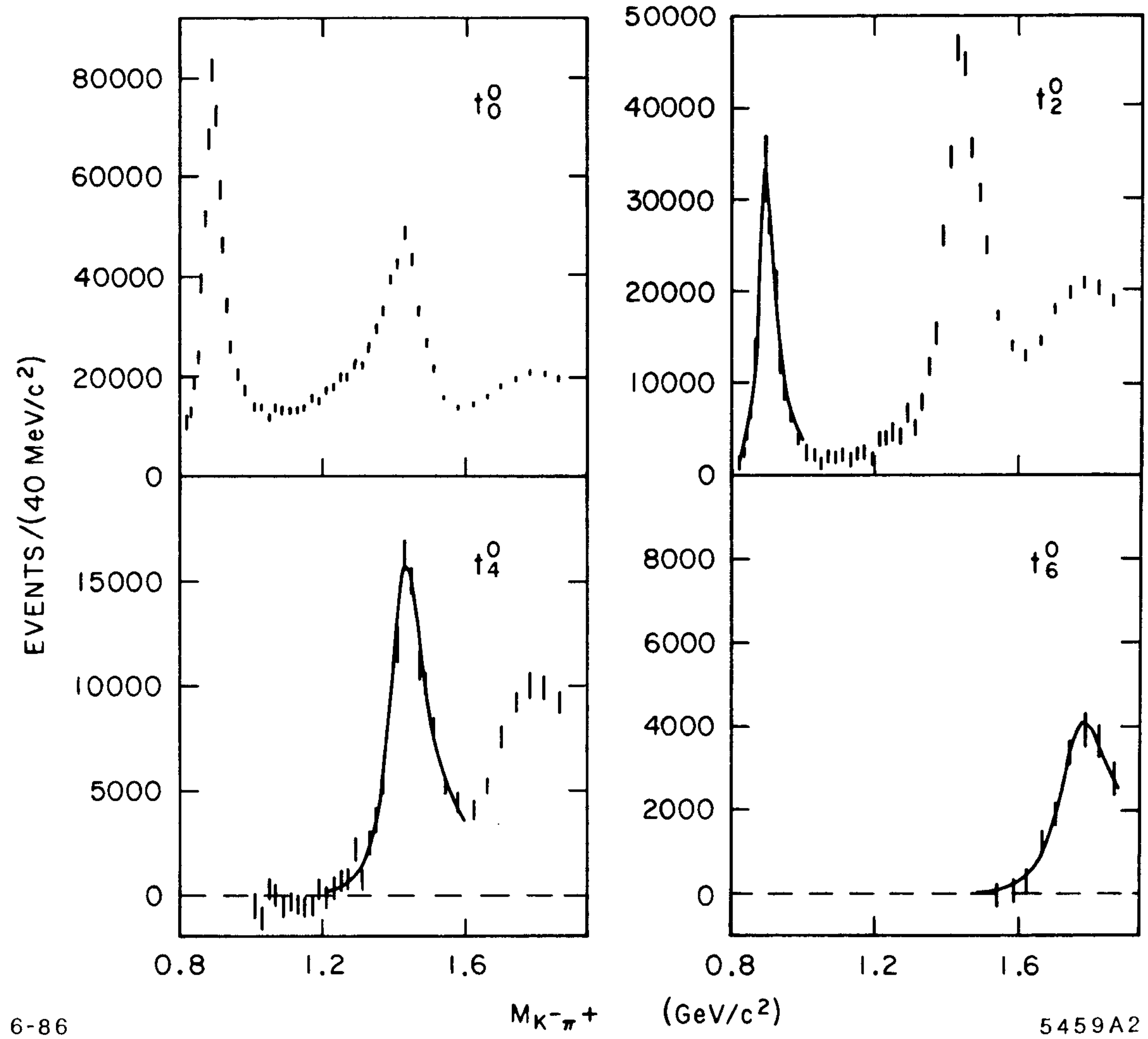

80000
60000
40000
20000
0
15000
10000
5000
0
50000
40000
30000
20000
10000
0
8000
6000
4000
2000
0
t_0^0
t_2^0
t_4^0
t_6^0
EVENTS/(40 MeV/c^2)
0.8
1.2
1.6
0.8
1.2
1.6
$M_{K^-\pi^+}$ (GeV/c^2)
6-86
5459A2

Fig. 3

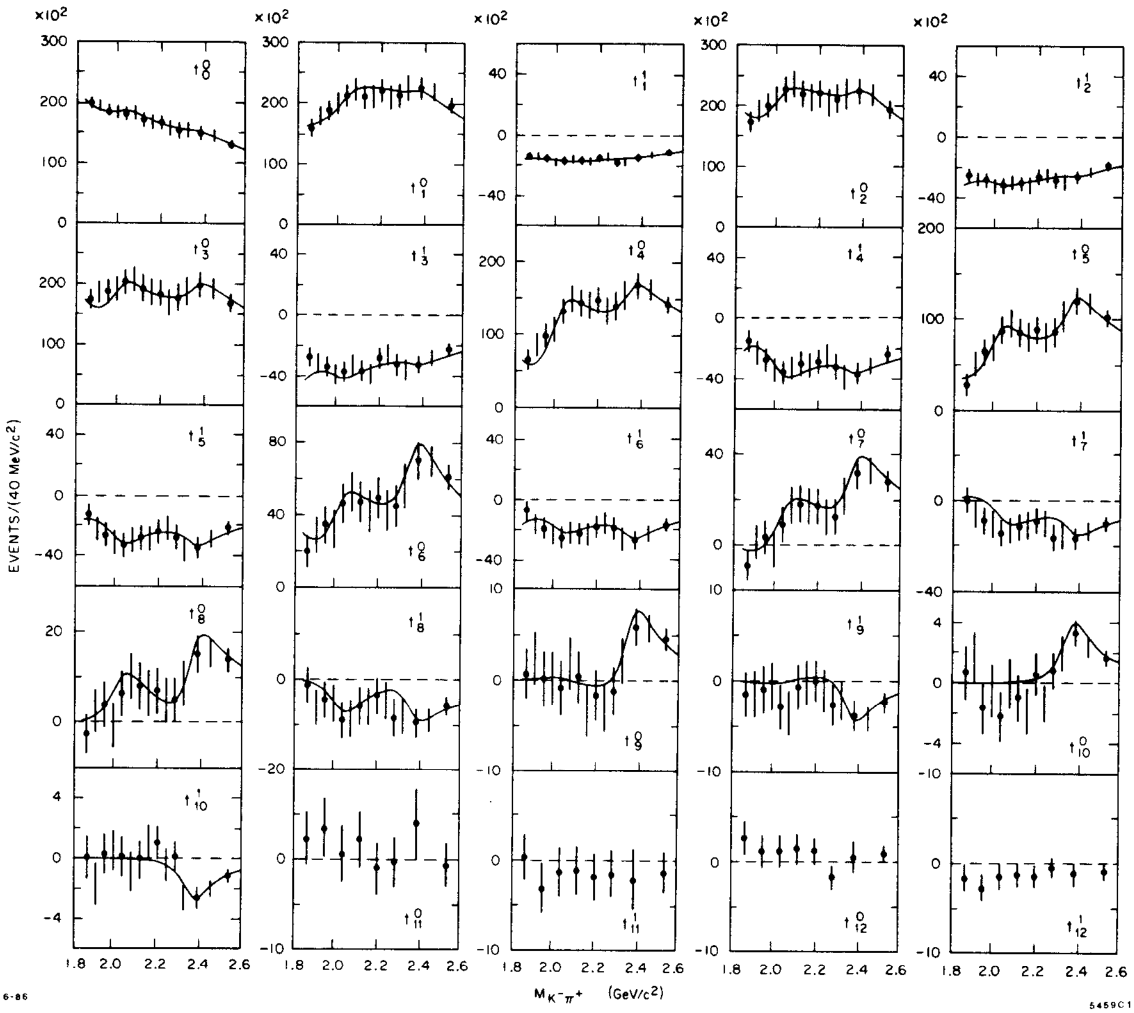

Fig. 4